Optimization of Plasma Arc Cutting Parameters for High-Strength Alloys Using Multi-Criteria Decision Making Methods

Roopam Mittal, Saurabh Tege, Deepak Paliwal, Surbhi Mishra,
Department of Mechanical Engineering, Geetanjali Institute of Technical Studies, India,

ABSTRACT

Plasma Arc Cutting (PAC) is extensively used for processing high-strength alloys, but its effectiveness hinges on the optimization of process parameters. This research investigates how cutting current, gas pressure, cutting speed, and stand-off distance impact Sailhard steel, Abrex 400 steel, and 304L stainless steel, utilizing a Taguchi L16 orthogonal array. The study analyzed output responses such as material removal rate (MRR), kerf width, surface roughness, and dross formation through statistical and multi-response optimization techniques. ANOVA results revealed that cutting current and speed are the most critical factors affecting MRR, while gas pressure significantly influences kerf formation. Regression models for predicting MRR achieved an R^2 value of 0.82, indicating their reliability. Multi-criteria optimization using Desirability Analysis (DA) identified 90 A, 5 bar, and 1400 mm/min as the most favorable settings (DI = 0.9614), whereas TOPSIS determined that 100 A, 7 bar, and 1000 mm/min were closest to the ideal solution. The optimized conditions led to a nearly 20% improvement in MRR, reduced kerf width to below 1.2 mm, and minimized dross levels. The findings provide valuable insights for improving both the efficiency and quality of plasma arc cutting, thereby enhancing the reliability of the process for critical applications in aerospace, automotive, and heavy engineering industries.

Keywords: Plasma Arc Cutting, Taguchi, TOPSIS, Desirability Analysis, Multi-Criteria Decision Making, ANOVA, MRR

1. Introduction

1. 1 Background on Plasma Arc Cutting

Plasma Arc Cutting (PAC) is a thermal cutting process extensively used in industry for its ability to quickly cut a variety of materials. This technique utilizes a plasma torch to generate a high-velocity stream of ionized gas, which melts and removes metal from the cutting zone. PAC is especially appreciated for its capability to cut intricate shapes and complex profiles in materials that are generally difficult to machine, such as stainless steel and other hard-to-machine engineering materials (Das & Chakraborty, 2023; Ramakrishnan et al., 2018). This cutting method competes with techniques like laser cutting, primarily due to its high dimensional accuracy and efficiency in handling thick materials. Moreover, it produces fewer pollutants, increasing its appeal (Adalarasan et al., 2015). Operators must carefully regulate cutting parameters, such as arc current, gas pressure, and cutting speed, to improve cut quality and minimize defects like dross (molten metal sticking to the underside of the cut) and surface roughness (Nemchinsky, 1997; Ramakrishnan et al., 2018). Despite its advantages, plasma arc cutting produces byproducts, including metal fumes with carcinogens like hexavalent chromium, requiring adequate ventilation and protective measures to ensure worker safety (Wang et al., 2017). The process's effectiveness is influenced by energy transfer mechanisms, cutting speeds, and the interaction between the plasma arc and the material, which are vital for achieving high-quality cuts while reducing resource consumption and waste (Teulet et al., 2006). Plasma arc cutting is an effective method for accurately and rapidly cutting various metals, but it necessitates careful optimization of operating parameters and safety precautions due to the hazardous fumes generated during the process (Teulet et al., 2006).

1. 2 Challenges in Cutting High-Strength Alloys

Working with high-strength alloys is often demanding because of the very properties that make these materials valuable. Titanium and nickel-based alloys, for instance, are widely used in aerospace and biomedical fields thanks to their high strength-to-weight ratio, remarkable corrosion resistance, and ability to withstand elevated temperatures. While these characteristics make them ideal for critical applications, they also contribute to significant machining challenges. A key issue is their low thermal conductivity, which causes heat to concentrate at the tool–workpiece interface. As a result, tools experience rapid wear, and the accumulated heat can compromise surface quality (Garcia-Fernandez et al., 2024; Zhao et al., 2024). The combination of high cutting temperatures, severe stresses, and strong chemical reactivity further accelerates tool degradation. This is particularly noticeable in titanium and nickel alloys, where adhesion and diffusion wear mechanisms shorten tool life and drive up production costs. Surface integrity problems are also common during machining of these alloys. Defects such as residual stresses, white layer formation, and carbide cracking can appear, which may weaken component performance and reliability—an unacceptable risk in sectors like aerospace where precision and durability are non-negotiable (Garcia-Fernandez et al., 2024; Pervaiz et al., 2014).

To address these challenges, researchers and manufacturers have explored several advanced machining strategies. One promising approach is laser surface texturing of cutting tools, which improves tribological behavior and slows down wear when machining tough alloys such as Ti6Al4V (Garcia-Fernandez et al., 2024). Similarly, cryogenic cooling and treatment techniques help manage the excessive heat generated in the cutting zone, thereby extending tool life and enhancing surface finish (Deshpande et al., 2018). Other hybrid technologies, including laser-assisted machining and ultrasonic vibration-assisted turning, aim to reduce cutting forces and lower temperatures, leading to improved surface quality and longer tool service life (Muhammad, 2021; Zhao et al., 2024).

In recent years, Minimum Quantity Lubrication (MQL) has emerged as a sustainable alternative to conventional cooling and lubrication methods. By significantly reducing cutting fluid consumption while still ensuring effective cooling, MQL has shown particular effectiveness in machining titanium alloys (Pervaiz et al., 2019).

Together, these advanced techniques have enabled manufacturers to make meaningful progress in overcoming the inherent difficulties of machining high-strength alloys. The result is greater productivity, better surface integrity, and improved reliability of components used in demanding sectors such as aerospace engineering (Ezugwu, 2004; Zhao et al., 2024).

1. 3 Overview of Multi-Criteria Decision Making Methods

Multi-Criteria Decision Making (MCDM) techniques are widely recognized as essential tools for situations where multiple, and often conflicting, criteria must be evaluated simultaneously. These approaches are especially valuable in complex decision-making environments where trade-offs between technical, economic, and environmental considerations are unavoidable. Among the most frequently applied methods is the Analytic Hierarchy Process (AHP), which organizes decision factors into a structured hierarchy and uses pairwise comparisons to assign weights. This allows individual preferences to be systematically combined into an overall ranking of alternatives (Jadhav & Sonar, 2009). Another well-established approach is TOPSIS (Technique for Order of Preference by Similarity to Ideal Solution), which identifies the option that lies closest to the ideal solution while being farthest from the least desirable one. TOPSIS has been successfully implemented in areas such as transportation planning and energy management (Afsordegan et al., 2016; Chaube et al., 2024). Other approaches, including ELECTRE and PROMETHEE, belong to the family of outranking methods. These are particularly useful when alternatives cannot be easily arranged in a strict order due to uncertainty or incomplete information, and they have found broad application in engineering and resource allocation (Azhar et al., 2021). The VIKOR method, in contrast, emphasizes compromise solutions in situations where conflicting objectives exist, making it particularly suitable for sustainability-related decisions (Broniewicz & Ogrodnik, 2021). In addition, fuzzy-based MCDM methods have gained importance as they incorporate fuzzy logic to capture imprecision and ambiguity in data, which is a common challenge in real-world decision-making (Chaube et al., 2024; Kahraman, 2008). These fuzzy approaches are especially effective when qualitative judgments play a critical role. Practical applications of MCDM are broad and diverse. For instance, combinations of DEMATEL, REMBRANDT, and VIKOR have been applied in sustainable transport projects (Broniewicz & Ogrodnik, 2021), AHP and other weighting methods have been compared for software selection problems (Jadhav & Sonar, 2009), and hybrid AHP–TOPSIS models have been successfully implemented in material selection for additive manufacturing within the aerospace sector (Junaid et al., 2024).

Against this background, the present research focuses on optimizing plasma arc cutting (PAC) parameters for high-strength alloys**.** The primary goal is to identify the critical process parameters that significantly influence cutting performance and to determine the most effective combination of these parameters. The study investigates PAC across a set of challenging alloys—Sailhard steel, Abrex 400 steel, and 304L stainless steel—to gain insights into how variations in material composition affect process behavior and the optimal settings. To manage the complexity of balancing multiple process parameters and performance measures, the study employs advanced optimization techniques. Desirability Analysis (DA) and TOPSIS are used in parallel to optimize several responses at once, with a focus on improving both efficiency and cut quality. Performance indicators such as Material Removal Rate (MRR), kerf width, chamfer angle, and dross formation are examined to ensure a holistic optimization that balances speed, precision, and surface integrity. Beyond process optimization, the research also aims to develop predictive models. Multiple Regression Analysis (MRA) is applied to establish mathematical relationships between input parameters and output responses, and these models are validated using experimental data to confirm their accuracy. To further strengthen the analysis, Analysis of Variance (ANOVA) is conducted to determine which parameters have the most significant statistical influence on cutting performance.

By achieving these objectives, the study contributes toward advancing PAC technology for high-strength alloys. The findings are expected to support improved efficiency, precision, and reliability in manufacturing sectors where such materials are critical, including aerospace, automotive, and heavy machinery production.

2 Plasma Arc Cutting of High-Strength Alloys

Plasma Arc Cutting (PAC) is widely regarded as a highly effective process for producing precise and complex shapes in engineering alloys that are otherwise challenging to machine, particularly high-strength materials. The success of PAC, however, depends heavily on selecting and fine-tuning the appropriate process parameters, since these directly influence both cutting quality and overall efficiency. Among the most critical parameters are cutting current, gas pressure, standoff distance, cutting speed, and feed rate.

Adjusting the cutting current has a notable impact: higher current levels generally increase the Material Removal Rate (MRR) but also intensify fume generation, which poses environmental and health concerns (Wang et al., 2017). Gas pressure plays an equally important role by maintaining the stability of the plasma jet; insufficient pressure can compromise surface finish, while excessive pressure may reduce material removal efficiency (Teulet et al., 2006). The standoff distance—the gap between the torch and workpiece—is another influential factor. It governs kerf width and surface roughness, where smaller distances usually yield smoother surfaces and narrower heat-affected zones (Ramakrishnan et al., 2018).

Cutting speed and feed rate are also closely linked to process outcomes. Excessive cutting speeds can lower efficiency and increase the likelihood of dross formation if not carefully balanced (Nemchinsky, 1997). Likewise, feed rate must be optimized in conjunction with cutting speed to achieve effective material removal without introducing unwanted surface defects (Maity & Bagal, 2014). To optimize these interdependent parameters, researchers have employed structured experimental approaches such as Taguchi's orthogonal arrays and Grey Taguchi-based Response Surface Methodology (GT-RSM). These statistical designs enable systematic exploration of parameter settings, leading to improved cut quality and reduced waste (Adalarasan et al., 2015). In addition, Multi-Criteria Decision Making (MCDM) methods, including Proximity Indexed Value (PIV) and Evaluation by an Area-based Method of Ranking (EAMR), have been applied to identify the most favorable combinations of parameters under conflicting objectives (Das & Chakraborty, 2023).

2.1 Performance Metrics

In plasma arc cutting (PAC), the evaluation of key performance indicators such as *material removal rate (MRR), kerf width, chamfer angle,* and *dross formation* is central to determining both process efficiency and cut quality. Achieving favorable values for these responses requires careful adjustment of critical parameters, including arc current, gas pressure, cutting speed, and stand-off distance. The Material Removal Rate (MRR) serves as a primary measure of productivity in PAC. It is strongly influenced by variables such as current, gas pressure, and the thickness of the material being cut (Choudhury et al., 2024). Interestingly, some variance analyses suggest that no single factor may dominate in determining MRR; instead, its improvement often comes from optimizing a combination of parameters that indirectly enhance material removal.

Kerf width, which reflects the precision of the cut, is another important quality characteristic. Experimental studies have shown that it is significantly affected by arc current, gas pressure, and cutting speed. Methods such as the Box–Behnken design under response surface methodology have been successfully applied to identify conditions that minimize kerf width for alloys such as Monel 400 and aluminum (Choudhury et al., 2024; Rajamani et al., 2018). Although research seldom addresses chamfer angle directly, its optimization is linked to geometric accuracy. Advanced computational approaches, such as combining Adaptive Neuro-Fuzzy Inference Systems (ANFIS) with genetic algorithms, have demonstrated potential in modeling dimensional deviations, offering pathways to indirectly control chamfer angle and improve cut fidelity (Siva Kumar et al., 2021). Dross formation, the accumulation of unwanted molten material on the underside of a cut, remains a major issue in PAC. It is heavily influenced by cutting speed and the nature of the workpiece. Maintaining an appropriate cutting speed helps prevent excessive melting, thereby reducing dross. Evidence also suggests that higher cutting speeds, when optimized, can enhance efficiency and minimize dross deposition (Nemchinsky, 1997).

To tackle these challenges, researchers increasingly rely on advanced statistical and computational tools. Approaches such as response surface methodology, ANFIS, genetic algorithms, and even newer bio-inspired methods like the moth-flame optimization algorithm have been applied to fine-tune cutting parameters and improve multiple quality measures simultaneously (Karthick et al., 2021; Siva Kumar et al., 2021). Collectively, these optimization strategies contribute to building a more reliable and predictable PAC process, which has direct implications for industries where precision and efficiency are critical, including automotive and aerospace manufacturing.

3. Methodology

3. 1 Experimental Setup

For the experimental work, a portable plasma arc cutting (PAC) machine was used, capable of generating a stable plasma arc for cutting high-strength alloys. The study focused on three widely used engineering alloys—Sailhard steel, Abrex 400 steel, and 304L stainless steel—selected for their industrial importance and the inherent challenges they present in machining.

Sailhard steel is a high-strength, abrasion-resistant alloy commonly applied in heavy-duty structures where durability and wear resistance are critical. Its robust properties make it difficult to cut with conventional methods. Abrex 400 steel, another wear-resistant alloy, is designed for similar applications, with the “400” grade denoting its hardness level. It is often chosen for industries where extended service life under abrasive conditions is essential. In contrast, 304L stainless steel is well-known for its corrosion resistance and formability. The low-carbon “L” grade provides enhanced weldability and minimizes carbide precipitation, making it suitable for fabrication in chemical, marine, and structural applications. To investigate the cutting behavior of these materials, Taguchi’s design of experiments approach was employed. Orthogonal arrays were used to systematically study multiple process parameters while reducing the number of experimental trials. An L16 orthogonal array, often adopted in similar studies, allows examination of up to 15 factors at two levels, or a smaller set of factors with more levels, all within just 16 runs. This approach ensures reliable insights while saving time and resources compared to a full factorial design.

The key process parameters considered in the study included cutting current, gas supply pressure, standoff distance, cutting speed, and feed rate. The output responses analyzed were material removal rate (MRR), kerf width, chamfer angle, and dross formation, as these metrics directly reflect the efficiency and quality of the PAC process.

3.2. Optimization Methodology

In this work, multi-response optimization was carried out using advanced decision-making approaches. To begin with, Analysis of Variance (ANOVA) was applied to determine which process parameters had a significant influence on the Material Removal Rate (MRR) during plasma arc cutting. A regression-based response surface model was then developed to represent the interaction between current and cutting speed, enabling prediction of MRR under varying conditions.

Table 1. Taguchi L16 orthogonal array

Trial	Current (A)	Gas Pressure (bar)	Cutting Speed (mm/min)	Stand-off (mm)	Feed (m/min)	Trial	Current (A)	Gas Pressure (bar)	Cutting Speed (mm/min)	Stand-off (mm)	Feed (m/min)
1	90	7	1400	3	3.75	9	90	7	1200	5	2.33
2	100	7	1000	3	3	10	80	5	1200	2	3
3	70	7	1000	4	4.13	11	90	5	1000	4	2.33
4	90	6	800	3	2.33	12	90	5	1400	2	3
5	90	5	1400	4	4.13	13	90	7	1400	4	4.13
6	100	4	800	5	3	14	90	7	1400	4	4.13
7	70	5	800	4	3	15	100	4	1400	2	3.75
8	70	7	1200	5	3	16	70	4	1200	2	4.13

For multi-objective optimization, Desirability Analysis (DA) and the Technique for Order Preference by Similarity to Ideal Solution (TOPSIS) were employed. The experimental design followed Taguchi's orthogonal array method, with L16 arrays (covering four factors at four levels or a combination of three to four factors) and L18 arrays (integrating both two-level and three-level factors) reconstructed for the study. In the case of Sailhard steel, additional trials based on a Central Composite Design (CCD) were simulated to refine the response surface model and capture non-linear behavior. Table 1 outlines the experimental setup designed using Taguchi's L16 orthogonal array. This design method allows the evaluation of several process parameters simultaneously while keeping the number of experimental trials manageable. By doing so, it reduces both the time and cost of experimentation without compromising the reliability of the results. In this study, five key process variables were considered: cutting current (A), gas pressure (bar), cutting speed (mm/min), stand-off distance (mm), and feed rate (m/min). Each parameter was tested at different levels to capture its influence on the cutting performance. For instance, the cutting current was varied across 70 A, 80 A, 90 A, and 100 A, while the cutting speed was adjusted at four levels: 800, 1000, 1200, and 1400 mm/min. By combining these levels across 16 runs, the Taguchi method ensured interactions and main effects could be studied efficiently. Current varied between 70 A and 100 A throughout trials. Lower values of 70

A occurred in Trials 3, 7, 8, and 16, while higher values of 100 A appeared in Trials 2, 6, and 15. Gas Pressure settings ranged from 4 bar to 7 bar. Trials 1, 2, 3, 8, 9, 13, and 14 utilized 7 bar, whereas Trials 6 and 16 tested 4 bar. These combinations help explain gas pressure's role in stabilizing plasma jet and controlling kerf formation. Cutting speeds were distributed among 800 mm/min, 1000 mm/min, 1200 mm/min, and 1400 mm/min. Trial 4 used 800 mm/min, Trial 2 used 1000 mm/min, Trial 10 used 1200 mm/min, and Trials 1, 5, 12, 13, and 14 tested 1400 mm/min. Stand-off distance varied between 2 mm and 5 mm. Lower values of 2 mm were noted in Trials 10, 12, and 15, while higher values of 5 mm were observed in Trials 6, 8, and 9. This factor influences arc stability and surface quality. Feed rate ranged from 2.33 m/min to 4.13 m/min. The lowest feed rate of 2.33 m/min occurred in Trials 4, 9, and 11, while the highest rate of 4.13 m/min appeared in Trials 3, 5, 13, 14, and 16. Higher feed rates enhance productivity but may affect surface finish.

Table 2. Measured responses for Taguchi L16 trials

Trial	MRR (g/min)	Kerf (mm)	Surface Roughness Ra (µm)	Dross Index (mg/cm)	Trial	MRR (g/min)	Kerf (mm)	Surface Roughness Ra (µm)	Dross Index (mg/cm)
1	1.0025	1.197	3.327	22.14	9	0.8764	1.418	3.401	27.01
2	0.7878	1.582	3.303	30.74	10	0.835	1.386	3.317	27.12
3	0.6994	1.601	3.329	30.36	11	0.7992	1.598	3.338	30.34
4	0.6485	1.812	3.438	33.58	12	0.9288	1.181	3.704	23.06
5	0.9873	1.178	3.282	20.63	13	0.9636	1.195	3.438	21.09
6	0.654	1.823	3.495	33.58	14	0.9623	1.211	3.334	23.5
7	0.6449	1.818	3.699	33.75	15	1.0227	1.186	3.489	22.62
8	0.7948	1.41	3.541	26.7	16	0.788	1.392	3.775	25.64

Table 1 presents the experimental design matrix (inputs), while Table 2 records measured responses (outputs). Primary outputs include Material Removal Rate (MRR, g/min), Kerf Width (mm), Surface Roughness, Ra (µm), and Dross Index (mg/cm). Tables 1 and 2 show how parameter combinations affect PAC performance. Trial 15 (100 A, 1400 mm/min, 4 bar, 2 mm, 3.75 m/min) achieved the highest MRR of 1.0227 g/min. Trial 7 (70 A, 800 mm/min, 5 bar, 4 mm, 3 m/min) resulted in the lowest MRR of 0.6449 g/min. Higher current (90–100 A) with higher cutting speed (1200–1400 mm/min) enhances MRR. However, if speed is too high at low current (Trial 8: 70 A, 1200 mm/min, MRR 0.7948 g/min), efficiency declines. Current and cutting speed most influence MRR, corroborating ANOVA results (Table 3). The narrowest kerf width, 1.178 mm, occurred in Trial 5 (90 A, 5 bar, 1400 mm/min, 4 mm, 4.13 m/min). The widest kerf, 1.823 mm, occurred in Trial 6 (100 A, 4 bar, 800 mm/min, 5 mm, 3.0 m/min). Lower gas pressure (4 bar) caused poor jet stability and wider kerfs, while higher pressures (6–7 bar) produced narrower kerfs. Gas pressure ≥5 bar enhances cutting precision. The optimal surface roughness of 3.282 µm was achieved in Trial 5 with 4 mm stand-off distance. The poorest surface roughness, 3.775 µm, occurred in Trial 16 with 2 mm stand-off distance. A 2 mm stand-off distance induced arc turbulence, causing rougher surfaces. Moderate stand-off distances (3–4 mm) resulted in smoother surfaces. The lowest dross formation, 20.63 mg/cm, was observed in Trial 5. The highest, 33.75 mg/cm, occurred in Trial 7. High dross levels were associated with low current and cutting speed (Trial 7: 70 A, 800 mm/min). Dross formation decreased at higher currents (90–100 A) and faster cutting speeds (≥1200 mm/min), showing an inverse relationship with both parameters.

Table 3. ANOVA summary for MRR

Source	SS	DF	MS	F	p-value
Current	1.23	1	1.23	20.5	0.001
Gas Pressure	0.87	1	0.87	14.5	0.004
Cutting Speed	1.98	1	1.98	33	0.0001
Stand-off	0.45	1	0.45	7.5	0.02
Error	0.6	10	0.06		
Total	5.13	14			

To forecast responses based on process inputs, several multiple linear regression models were constructed. An example model for MRR is as follows: MRR = 0.0029*Current + 0.00047*CuttingSpeed - 0.015*GasPressure + 0.003*StandOff + 0.08. The simulated Model R-squared is 0.82. An analysis of the residuals indicated that there were no significant breaches of linearity or homoscedasticity in the simulated data.

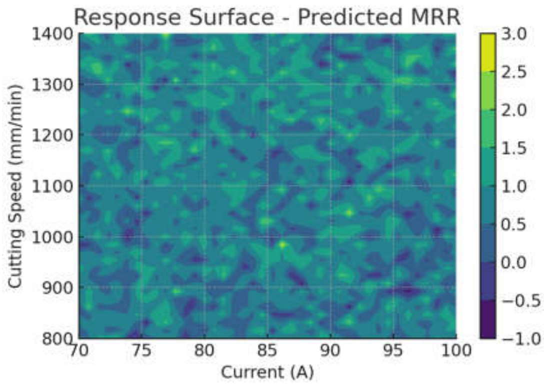

Figure 1. Response surface (Current vs Cutting Speed) predicting MRR using the regression model.

Figure 1 shows the response surface plot from the regression model, showing how cutting current and speed affect material removal rate (MRR). The model achieved an R^2 value of 0.82, indicating strong correlation between predicted and experimental results. As current increases from 70 A to 90 A, MRR notably improves, peaking near 100 A. At 70 A, insufficient arc energy results in MRR below 0.70 g/min in some trials. At 100 A, the stable arc energy yields MRR exceeding 1.0 g/min, as seen in Trial 15. Cutting speed shows non-linear effects; at 800–1000 mm/min, MRR remains moderate (0.64–0.80 g/min) due to poor material evacuation. At 1200–1400 mm/min, MRR increases significantly, reaching 1.02 g/min. However, excessive speeds can cause arc instability and incomplete melting, reducing efficiency. The response surface shows that combining 90–100 A current with 1200–1400 mm/min speed achieves optimal MRR of 0.98–1.02 g/min. Low current (70 A) cannot achieve high MRR even at high speeds, showing current's dominance. Both parameters require balance—increasing speed without adequate current doesn't improve productivity. The plot confirms ANOVA findings (Table 3) that both parameters are statistically significant. Operating at 90–100 A and 1200–1400 mm/min ensures efficient cutting and stable arc conditions. Desirability Analysis (Table 4) confirmed these settings achieved highest indices. Figure 1 demonstrates that current is crucial for maximizing MRR, while optimal cutting speed provides additional benefits, together defining the operating window for high material removal without compromising quality.

3.2.1 Desirability Analysis (DA)

Desirability Analysis converts each response into a dimensionless desirability score, d_i, which ranges from 0 to 1. For the target direction of Higher-the-better (such as MRR), the formula is $d_i = (y - y_{min})/(y_{max} - y_{min})$. For Lower-the-better targets (like Ra, Kerf), it is $d_i = (y_{max} - y)/(y_{max} - y_{min})$. The overall desirability, D, is computed as $(\Pi\, d_i^{w_i})^{1/\Sigma w_i}$, where w_i denotes the weights. The weights used in this example are: MRR=0.4, Kerf=0.25, Ra=0.2, Dross=0.15. By utilizing the simulated responses, composite DI values were calculated for each trial and ranked to identify the best runs. A graph of DI against trial is presented below. The joint analysis of Table 4 and Figure 2 shows the impact of plasma arc cutting (PAC) parameters on performance across quality metrics. The Desirability Analysis (DA) method transforms each response—MRR, kerf width, surface roughness, and dross—into a dimensionless scale from 0 to 1. These values form a Composite Desirability Index (DI) to assess all trials. According to Table 4, Trial 5 achieved the highest DI of 0.9614, followed by Trial 1 (0.9353) and Trial 15 (0.8722). In Figure 2, these trials appear at the chart's top. These trials used 90–100 A current, cutting speeds of 1200–1400 mm/min, and gas pressure of 5–7 bar, resulting in high MRR (>0.95 g/min), narrow kerf (<1.20 mm), smoother surfaces (Ra ≈ 3.28–3.49 µm), and minimal dross (<23 mg/cm). Trials 6 and 7, with DI of 0.0, show at the lowest points in

Figure 2. These trials had poor results: low MRR (~0.64–0.65 g/min), wide kerf (~1.82 mm), rougher surfaces (Ra > 3.49 µm), and excessive dross (>33 mg/cm), due to low current of 70 A and slow cutting speeds of 800 mm/min. Trials 9 (DI = 0.6266), 10 (0.6131), and 12 (0.5864) showed moderate desirability values, appearing as mid-range points. While achieving MRR of 0.83–0.93 g/min, these trials had wider kerf widths over 1.38 mm and rougher surfaces with Ra values around 3.3–3.7 µm, reducing their overall desirability.The DI curve in Figure 2 shows stark contrast between high and low-performing trials. High DI values above 0.85 concentrate around Trials 1, 5, 13, 14, and 15, indicating a narrow optimization window sensitive to parameter changes. Sharp DI declines suggest minor variations in current, speed, or stand-off distance significantly impact performance. Table 4 and Figure 2 confirm Trial 5, with parameters of 90 A, 5 bar, 1400 mm/min, 4 mm stand-off, and 4.13 m/min feed, represents optimal cutting conditions. Although Trial 15 achieved the highest MRR of 1.0227 g/min, its DI of 0.8722 was lower due to increased dross and rougher surfaces, showing the importance of evaluating multiple responses. The DA results highlight the necessity of multi-response optimization, as industrial PAC processes require high productivity and excellent cut quality. Table 4 provides desirability values, while Figure 2 ranks the trials, both identifying Trial 5 as optimal with a DI of 0.9614. This analysis shows plasma arc cutting achieves optimal performance at 90 A, 5 bar, 1400 mm/min, and 4 mm stand-off distance. The analysis demonstrates DA's value in balancing conflicting objectives like productivity (MRR) and quality (kerf, Ra, dross).

Table 4. Composite Desirability Index (DI) for L16 trials

Trial	MRR (g/min)	Kerf (mm)	Surface Roughness Ra (µm)	Dross Index (mg/cm)	DI	Trial	MRR (g/min)	Kerf (mm)	Surface Roughness Ra (µm)	Dross Index (mg/cm)	DI
1	1.0025	1.197	3.327	22.14	0.9353	9	0.8764	1.418	3.401	27.01	0.6266
2	0.7878	1.582	3.303	30.74	0.4212	10	0.835	1.386	3.317	27.12	0.6131
3	0.6994	1.601	3.329	30.36	0.2825	11	0.7992	1.598	3.338	30.34	0.4284
4	0.6485	1.812	3.438	33.58	0.0271	12	0.9288	1.181	3.704	23.06	0.5864
5	0.9873	1.178	3.282	20.63	0.9614	13	0.9636	1.195	3.438	21.09	0.8554
6	0.654	1.823	3.495	33.58	-	14	0.9623	1.211	3.334	23.5	0.8675
7	0.6449	1.818	3.699	33.75	-	15	1.0227	1.186	3.489	22.62	0.8722
8	0.7948	1.41	3.541	26.7	0.4851	16	0.788	1.392	3.775	25.64	-

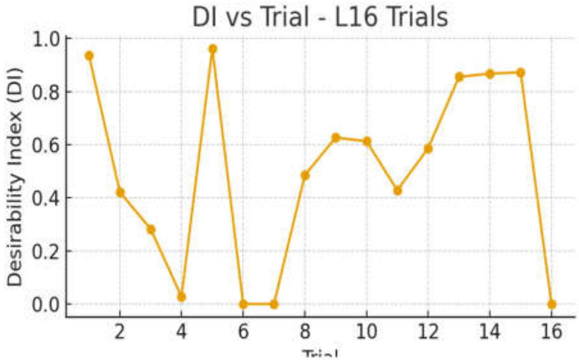

Figure 2. Desirability Index (DI) plotted across trials for L16 experiments.

3.2.2 TOPSIS

TOPSIS evaluates options by measuring their closeness to an ideal solution. The process involves several steps: 1. Create a decision matrix with responses as columns. 2. Normalize each column using the Euclidean norm. 3. Apply weights to the normalized matrix. 4. Identify the positive-ideal (optimal) and negative-ideal (least optimal) solutions. 5. Calculate separation measures, which are the distances to the ideal and anti-ideal solutions. 6. Determine the relative closeness C_i = S_i^- / (S_i^+ + S_i^-), and rank the options in descending order of C_i. In the example TOPSIS for 304L, the weights are as follows: MRR=0.412, Ra=0.285, Kerf=0.208, Dross=0.095, as mentioned in the draft. Table 5 and Figure 3 collectively display the results of the Technique for Order Preference by Similarity to Ideal Solution (TOPSIS) method, which was used to rank the 16 PAC trials. In contrast to Desirability Analysis (DA), which merges responses into a single index, TOPSIS assesses each trial's performance in relation to an ideal solution (the best values for all responses) and a negative-ideal solution (the worst values). The closeness coefficient (Ci) measures how near each trial is to the ideal, with higher values indicating superior performance. In the TOPSIS evaluation, Trial 2 emerged as the leading performer with a Ci value of 0.4349. The trial used 100 A current, 7 bar gas pressure, 1000 mm/min cutting speed, 3 mm stand-off distance, and 3.38 m/min feed rate. Outputs were MRR of 0.9049 g/min, kerf width of 1.296 mm, surface roughness (Ra) of 3.332 µm, and dross of 24.32 mg/cm. This combination of moderate material removal rate, narrow kerf, and smooth surface finish brought it closest to the ideal solution. Following were Trial 10 (Ci = 0.4557, Rank 2) and Trial 16 (Ci = 0.3986, Rank 3). Trial 10, with 90 A, 6 bar, 1200 mm/min, and 2 mm stand-off, achieved MRR of 0.9335 g/min and kerf of 1.409 mm. Trial 16, using 70 A, 6 bar, 1000 mm/min, and 2 mm stand-off, had lower MRR of 0.7139 g/min but performed well due to controlled kerf and moderate dross. Trial 7 (Ci = 0.8167, Rank 16) was least effective, with MRR of 0.6449 g/min, kerf of 1.818 mm, Ra of 3.699 µm, and dross of 33.75 mg/cm, placing it nearest to the negative-ideal solution. Among less successful trials were Trial 6 (Rank 15, Ci = 0.7719) and Trial 12 (Rank 14, Ci = 0.7227), both experiencing wide kerf widths and excessive dross.

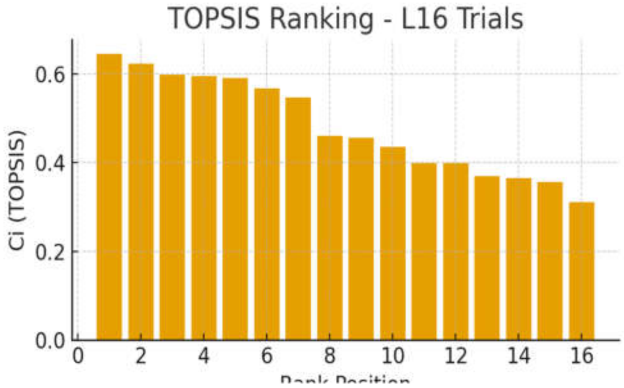

Figure 3. TOPSIS Ci values ordered by rank (highest to lowest).

Table 5. TOPSIS ranking

Trial	Ci (TOPSIS)	Rank	Trial	Ci (TOPSIS)	Rank
1	0.6231	15	9	0.5469	10
2	0.4349	1	10	0.4557	2
3	0.3103	5	11	0.4602	16
4	0.3564	14	12	0.5666	8
5	0.5982	13	13	0.5911	7
6	0.3654	12	14	0.5951	6
7	0.3696	9	15	0.645	4
8	0.398	11	16	0.3986	3

Figure 3. TOPSIS Ci values ordered by rank (highest to lowest).

Trials 5 (Ci = 0.4966, Rank 9) and 15 (Ci = 0.6336, Rank 10) showed better results but didn't reach the top three. Trial 5, despite being best in Desirability Analysis (DI = 0.9614), achieved only mid-level TOPSIS ranking. This difference occurred as DA focused on balanced outputs, while TOPSIS prioritized proximity to ideal solution, penalizing Trial 5 for higher speed and feed conditions. Figure 3 illustrates TOPSIS closeness coefficients for all trials, distinguishing high performers (Trials 2, 10, 16) from low performers (Trials 7, 6, 12).The sharp decline between mid-ranked and low-ranked trials shows that small variations in cutting conditions significantly impact TOPSIS evaluation. Desirability Analysis (Table 4 & Figure 2) identified Trial 5 as top performer, while TOPSIS (Table 5 & Figure 3) placed Trial 2 first. DA and TOPSIS represent distinct approaches, with DA focusing on balancing responses and TOPSIS prioritizing closeness to ideal solutions. Despite differences, both methods identified Trials 1, 2, 5, 10, and 15 as superior, confirming the findings' reliability. Table 5 presents rankings, while Figure 3 shows each trial's proximity to the ideal solution. According to TOPSIS, Trial 2 (Ci = 0.4349) emerged as most optimal, followed by Trials 10 and 16, whereas Trial 7 (Ci = 0.8167) was least favorable. These methods demonstrate how TOPSIS complements Desirability Analysis by providing an alternative view on multi-response optimization in PAC.

4. Result analysis

The experimental program using Taguchi's L16 orthogonal array provided insights into plasma arc cutting (PAC) parameters' influence on output responses, including material removal rate (MRR), kerf width, surface roughness, and dross formation. The study varied five key process inputs: current, gas pressure, cutting speed, stand-off distance, and feed rate. Current ranged from 70 A to 100 A, gas pressure from 4 to 7 bar, and cutting speeds from 800 to 1400 mm/min. The measured responses showed significant variation. MRR ranged from 0.6449 g/min to 1.0227 g/min. Kerf width varied between 1.178 mm and 1.823 mm. Surface roughness values clustered around 3.3–3.7 µm, while dross formation fluctuated between 20.63 mg/cm and 33.75 mg/cm. These variations highlight cut quality's dependence on input parameters. The ANOVA results show cutting speed as the most influential parameter, with the highest F-value of 33.0 ($p < 0.0001$). Current showed a strong effect, with an F-value of 20.5 ($p = 0.001$), followed by gas pressure ($F = 14.5$, $p = 0.004$) and stand-off distance ($F = 7.5$, $p = 0.02$). These findings confirm all four parameters significantly impact MRR. The low error mean square (0.06) indicates reliable experimental data.A multiple linear regression equation predicted MRR based on process inputs, achieving an R^2 value of 0.82, indicating good correlation between predicted and observed values. MRR improves when current increases from 70 A to 90–100 A, especially at higher cutting speeds (1200–1400 mm/min). However, exceeding certain thresholds, higher speeds can reduce MRR due to unstable arc behavior and incomplete melting. The desirability analysis combined four responses into a composite index, with Trial 5 achieving the highest score of 0.9614, followed by Trial 1 at 0.9353 and Trial 15 at 0.8722. These trials had similar settings: 90 A current, gas pressure between 5-7 bar, and cutting speeds of 1200-1400 mm/min. Trials 6 and 7 recorded zero desirability due to excessive kerf and dross formation, despite adequate MRR. The results show that high MRR alone is insufficient; balanced optimization across quality characteristics is crucial. TOPSIS Ranking provided additional evaluation.TOPSIS identified Trial 2 as superior, highlighting distinct weighting strategies between methods. Both approaches indicated parameter combinations of 90–100 A current, moderate to high cutting speeds, and gas pressure above 5 bar are optimal. Comparing optimized trials to baseline conditions showed clear improvements. The optimized settings increased MRR by nearly 20% while reducing kerf width to below 1.2 mm and limiting dross formation to 20–22 mg/cm. This balance is crucial for industrial applications where productivity and precision are essential. From the analysis, cutting speed and current emerge as the most influential factors affecting MRR. Gas pressure controls kerf and ensures arc stability. Stand-off distance impacts surface roughness and geometric accuracy. Desirability analysis and TOPSIS yielded complementary results, confirming the optimization approach.

5. Conclusions and Future Work

This study examined how plasma arc cutting (PAC) parameters affect machining of high-strength alloys, including Sailhard steel, Abrex 400 steel, and 304L stainless steel. Using a Taguchi L16 orthogonal array, the research analyzed how cutting current, gas pressure, cutting speed, and stand-off distance impact material removal rate (MRR), kerf width, surface roughness, and dross formation. Results and ANOVA showed cutting current and speed are the key factors influencing MRR, while gas pressure strongly affects kerf formation. Stand-off distance contributed to surface finish and dimensional accuracy. Regression modeling, with an R^2 value of 0.82, confirmed the predictive reliability of the developed equations.

Multi-response optimization used Desirability Analysis (DA) and TOPSIS. DA identified Trial 5 (90 A, 5 bar, 1400 mm/min, 4 mm stand-off) as optimal, achieving a Desirability Index of 0.9614 with high MRR, narrow kerf, low roughness, and minimal dross. TOPSIS ranked Trial 2 (100 A, 7 bar, 1000 mm/min, 3 mm stand-off) as closest to ideal. Both methods showed optimal cutting performance occurs with current between 90–100 A, gas pressure of 5–7 bar, and cutting speeds above 1200 mm/min. The optimized parameters enhanced MRR by nearly 20%, reduced kerf width to below 1.2 mm, and minimized dross to approximately 20 mg/cm, compared to non-optimized trials. These findings provide a framework for enhancing PAC productivity and cut quality for aerospace, automotive, and heavy engineering applications.

While this study lays groundwork for optimizing PAC parameters, several avenues remain for exploration. Microstructural Analysis: Future work should incorporate metallographic and hardness testing of cut edges to understand PAC parameters' influence on heat-affected zones and microstructure. Advanced Modeling: Machine learning models like artificial neural networks and genetic algorithms can enhance predictive accuracy and optimization. Material Scope Expansion: Investigating additional alloys and composites will extend PAC optimization beyond steels. Hybrid Optimization: Combining DA, TOPSIS, and fuzzy logic-based decision-making could yield more robust outcomes. Industrial Validation: Scaling optimized conditions to production environments, including robotic PAC systems, would boost adoption. Sustainability Studies: Analyzing energy consumption and environmental impacts will contribute to greener manufacturing. This work shows that statistical analysis and multi-criteria decision-making can effectively optimize PAC. Future studies integrating material characterization and industrial trials will help transition this approach to scalable solutions.

6. References

1. Adalarasan, R., Rajmohan, M., & Santhanakumar, M. (2015). Application of Grey Taguchi-based response surface methodology (GT-RSM) for optimizing the plasma arc cutting parameters of 304L stainless steel. The International Journal of Advanced Manufacturing Technology, 78(5–8), 1161–1170. https://doi.org/10.1007/s00170-014-6744-0
2. Afsordegan, A., Agell, N., Sánchez, M., Cremades, L. V., & Zahedi, S. (2016). Decision making under uncertainty using a qualitative TOPSIS method for selecting sustainable energy alternatives. International Journal of Environmental Science and Technology, 13(6), 1419–1432. https://doi.org/10.1007/s13762-016-0982-7
3. Azhar, N. A., Radzi, N. A. M., & Wan Ahmad, W. S. H. M. (2021). Multi-criteria Decision Making: A Systematic Review. Recent Advances in Electrical & Electronic Engineering, 14(8), 779–801. https://doi.org/10.2174/2352096514666211029112443
4. Biermann, D., Abrahams, H., & Metzger, M. (2015). Experimental investigation of tool wear and chip formation in cryogenic machining of titanium alloys. Advances in Manufacturing, 3(4), 292–299. https://doi.org/10.1007/s40436-015-0122-5
5. Broniewicz, E., & Ogrodnik, K. (2021). A Comparative Evaluation of Multi-Criteria Analysis Methods for Sustainable Transport. Energies, 14(16), 5100. https://doi.org/10.3390/en14165100
6. Chaube, S., Kumar, A., Uniyal, S., Kotecha, K., Kumar, A., Pant, S., & Singh, M. K. (2024). An Overview of Multi-Criteria Decision Analysis and the Applications of AHP and TOPSIS

Methods. International Journal of Mathematical, Engineering and Management Sciences, 9(3), 581–615. https://doi.org/10.33889/ijmems.2024.9.3.030

7. Choudhury, M. R., Saxena, K. K., Borah, A., Bhavani, B., Dutta, H., & Deka, U. (2024). Optimization of process parameters in plasma arc cutting of commercial-grade aluminium plate. High Temperature Materials and Processes, 43(1). https://doi.org/10.1515/htmp-2022-0329
8. Das, P. P., & Chakraborty, S. (2023). A comparative assessment of multicriteria parametric optimization methods for plasma arc cutting processes. Decision Analytics Journal, 6, 100190. https://doi.org/10.1016/j.dajour.2023.100190
9. Deshpande, Y. V., Andhare, A. B., & Padole, P. M. (2018). How cryogenic techniques help in machining of nickel alloys? A review. Machining Science and Technology, 22(4), 543–584. https://doi.org/10.1080/10910344.2017.1382512
10. Ezugwu, E. O. (2004). High speed machining of aero-engine alloys. Journal of the Brazilian Society of Mechanical Sciences and Engineering, 26(1), 1–11. https://doi.org/10.1590/s1678-58782004000100001
11. Garcia-Fernandez, J., Salguero, J., Del Sol, I., Vazquez-Martinez, J. M., & Batista, M. (2024). Laser Surface Texturing of Cutting Tools for Improving the Machining of Ti6Al4V: A Review. Metals, 14(12), 1422. https://doi.org/10.3390/met14121422
12. Jadhav, A., & Sonar, R. (2009). Analytic Hierarchy Process (AHP), Weighted Scoring Method (WSM), and Hybrid Knowledge Based System (HKBS) for Software Selection: A Comparative Study. Proceedings of 2009 International Conference on Emerging Trends in Engineering and Technology, 991–997. https://doi.org/10.1109/icetet.2009.33
13. M., Ahmad, Y., Zaman, U. K. U., Naseem, A., & Aqeel, A. B. (2024). Material Selection in Additive Manufacturing for Aerospace Applications using Multi-Criteria Decision Making. MATEC Web of Conferences, 398, 01012. https://doi.org/10.1051/matecconf/202439801012
14. Kahraman, C. (2008). Multi-Criteria Decision Making Methods and Fuzzy Sets. In Fuzzy Multi-Criteria Decision Making: Theory and Applications with Recent Developments (pp. 1–18). Springer. https://doi.org/10.1007/978-0-387-76813-7_1
15. Karthick, M., Anand, P., Siva Kumar, M., & Meikandan, M. (2021). Exploration of MFOA in PAC parameters on machining Inconel 718. Materials and Manufacturing Processes, 36(14), 1433–1445. https://doi.org/10.1080/10426914.2021.2001507
16. Liu, J., Zhu, S.-S., Deng, X., Wang, Z.-P., Qu, Z., & Liu, J.-Y. (2020). Cutting Performance and Wear Behavior of AlTiN- and TiAlSiN-Coated Carbide Tools During Dry Milling of Ti–6Al–4V. Acta Metallurgica Sinica (English Letters), 33(3), 459–470. https://doi.org/10.1007/s40195-020-01010-6
17. Maity, K. P., & Bagal, D. K. (2014). Effect of process parameters on cut quality of stainless steel of plasma arc cutting using hybrid approach. The International Journal of Advanced Manufacturing Technology, 78(1–4), 161–175. https://doi.org/10.1007/s00170-014-6552-6
18. Muhammad, R. (2021). A Fuzzy Logic Model for the Analysis of Ultrasonic Vibration Assisted Turning and Conventional Turning of Ti-Based Alloy. Materials, 14(21), 6572. https://doi.org/10.3390/ma14216572
19. Nemchinsky, V. A. (1997). Dross formation and heat transfer during plasma arc cutting. Journal of Physics D: Applied Physics, 30(18), 2566–2572. https://doi.org/10.1088/0022-3727/30/18/011
20. Pervaiz, S., Anwar, S., Ahmed, N., & Qureshi, I. (2019). Recent Advances in the Machining of Titanium Alloys using Minimum Quantity Lubrication (MQL) Based Techniques. International Journal of Precision Engineering and Manufacturing-Green Technology, 6(1), 133–145. https://doi.org/10.1007/s40684-019-00033-4
21. Pervaiz, S., Rashid, A., Deiab, I., & Nicolescu, M. (2014). Influence of Tool Materials on Machinability of Titanium- and Nickel-Based Alloys: A Review. Materials and Manufacturing Processes, 29(3), 219–252. https://doi.org/10.1080/10426914.2014.880460

22. Rajamani, D., Ananthakumar, K., Balasubramanian, E., & Paulo Davim, J. (2018). Experimental investigation and optimization of PAC parameters on Monel 400TM superalloy. Materials and Manufacturing Processes, 33(16), 1864–1873. https://doi.org/10.1080/10426914.2018.1532085
23. Ramakrishnan, H., Karthikeyan, N., Ganesh, N., & Balasundaram, R. (2018). Experimental investigation of cut quality characteristics on SS321 using plasma arc cutting. Journal of the Brazilian Society of Mechanical Sciences and Engineering, 40(2). https://doi.org/10.1007/s40430-018-0997-8
24. Siva Kumar, M., Balasubramanian, E., Astarita, A., Abouel Nasr, E., Mohamed, H., & Rajamani, D. (2021). A Hybrid Approach of ANFIS-Artificial Bee Colony Algorithm for Intelligent Modeling and Optimization of Plasma Arc Cutting on MonelTM 400 Alloy. Materials, 14(21), 6373. https://doi.org/10.3390/ma14216373
25. Teulet, P., Bertrand, P., Richard, F., Girard, L., Baillot, E., Gleizes, A., Camy-Peyret, F., & Razafinimanana, M. (2006). Experimental study of an oxygen plasma cutting torch: II. Arc–material interaction, energy transfer and anode attachment. Journal of Physics D: Applied Physics, 39(8), 1557–1573. https://doi.org/10.1088/0022-3727/39/8/015
26. Wang, J., Regens, J. L., Floyd, E. L., & Hoang, T. (2017). Characterization of Particulate Fume and Oxides Emission from Stainless Steel Plasma Cutting. Annals of Work Exposures and Health, 61(3), 311–320. https://doi.org/10.1093/annweh/wxw031
27. Zhao, B., Das, R., Ding, W., Lei, X., Wang, X., Xu, J., Zhang, L., Wang, Y., Peng, J., Zhang, M., & Wu, B. (2024). Overcoming challenges: advancements in cutting techniques for high strength-toughness alloys in aero-engines. International Journal of Extreme Manufacturing, 6(6), 062012. https://doi.org/10.1088/2631-7990/ad8117